Controlling dynamical quantum phase transitions

D. M. Kennes,[1] D. Schuricht,[2] and C. Karrasch[1]
[1]*Dahlem Center for Complex Quantum Systems and Fachbereich Physik, Freie Universität Berlin, 14195 Berlin, Germany*
[2]*Institute for Theoretical Physics, Center for Extreme Matter and Emergent Phenomena, Utrecht University, Princetonplein 5, 3584 CE Utrecht, The Netherlands*

(Received 25 March 2018; revised manuscript received 29 April 2018; published 10 May 2018)

We study the dynamics arising from a double quantum quench where the parameters of a given Hamiltonian are abruptly changed from being in an equilibrium phase A to a different phase B and back (A → B → A). As prototype models, we consider the (integrable) transverse Ising field as well as the (nonintegrable) ANNNI model. The return amplitude features nonanalyticities after the first quench through the equilibrium quantum critical point (A → B), which is routinely taken as a signature of passing through a so-called dynamical quantum phase transition. We demonstrate that nonanalyticities after the second quench (B → A) can be avoided and reestablished in a recurring manner upon increasing the time T spent in phase B. The system retains an infinite memory of its past state, and one has the intriguing opportunity to control at will whether or not dynamical quantum phase transitions appear after the second quench.

DOI: 10.1103/PhysRevB.97.184302

I. INTRODUCTION

In the last two decades we have witnessed an impressive surge in experimental advances pushing the frontier of realizing and controlling (effectively) closed nonequilibrium quantum many-body systems [1–3]. This is of fundamental importance, as the consequences of quantum many-body physics are observably real in these systems as well as of practical relevance as they might pave the way to quantum technologies in the future.

Two quantities that have recently attracted a tremendous amount of attention are the return amplitude [4],

$$G(t) = \langle \Psi_0 | e^{-iHt} | \Psi_0 \rangle, \tag{1}$$

and its related rate function,

$$l(t) = -\frac{1}{L} \ln |G(t)|^2. \tag{2}$$

Here $|\Psi_0\rangle$ is some initial state, usually taken to be the ground state of some Hamiltonian H_0, while the subsequent time evolution is governed by a different Hamiltonian H, a setup that is referred to as a quantum quench [5]. Intuitively, one might think of the square of the return amplitude as the probability of the ground state to return to itself under the time evolution with H.

As has been pointed out by Heyl *et al.* [6], the rate function (2) in the transverse-field Ising chain shows nonanalytic behavior at "critical times" t_n^*, provided the quantum quench has crossed the quantum critical point, i.e., if the ground states of the Hamiltonians H_0 and H belong to different zero-temperature phases. The appearance of these critical times signals the breakdown of a Taylor expansion in time. Heyl *et al.* also pointed out the mathematical analogy of the nonanalyticities in the rate function as well as the manifestation of an equilibrium phase transition in the usual free energy, and in doing so motivating the introduction of the term dynamical quantum phase transition (DQPT) for the former.

One of the hallmarks of equilibrium quantum phase transitions is the inability to adiabatically connect the ground state of one phase to the ground state of the other phase (of different symmetry). Therefore, a nonanalyticity in the ground-state energy is routinely encountered when passing between the phases, irrespective of the path chosen to achieve this crossing. In contrast, the robustness of DQPTs is much less clear. The appearance of DQPTs often [7–9] but not always [10–12] coincides with whether or not a quantum critical point separates H and H_0. Nevertheless, the further study of DQPTs has attracted a lot of theoretical interest [13–38] as well as successful efforts to realize DQPTs in ionic [39] and atomic [40] systems in optical lattices.

In this paper, we add to this debate a surprising flexibility in controlling DQPTs by performing double quenches (within the free transverse-field Ising chain and a nonintegrable generalization thereof). We elaborate on how the appearance of DQPTs can be tuned simply by increasing the time between the first and second quench. In particular, we show that the system can exhibit all four combinations of absence or presence of nonanalyticities before and after the second quench, respectively, as is illustrated for double quenches in the transverse-field Ising chain in Fig. 1. This not only suggests that the appearance of DQPTs is very fragile, but also indicates an intriguing long-term memory of the system. With this fragility in mind and motivated by recent experiments [39], we comment on the relation between nonanalyticities in the rate function and the time evolution of the magnetization. We find that the correspondence of zeros in the magnetization to the critical times t_n^*, observed earlier for the transverse-field Ising model [6], does not survive in the double-quench setup (similarly to when integrability-breaking terms are included [7] in a single-quench setup). This provides further evidence that the correspondence found for a single quench in the free case seems to be accidental.

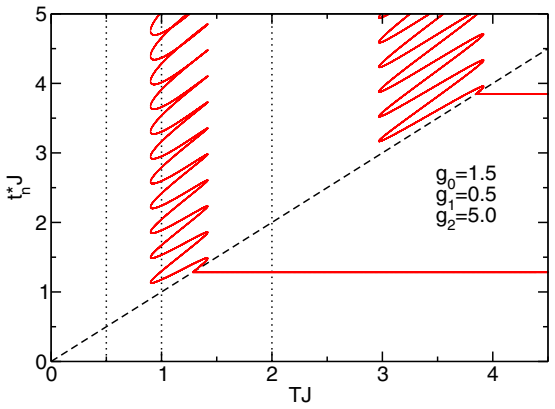

FIG. 1. Location of the critical times t_n^* in the t-T-plane for a double quench between the PM $\rightarrow$ FM $\rightarrow$ PM phases of the transverse-field Ising chain (quench parameters $g_0 = 1.5$, $g_1 = 0.5$ and $g_2 = 5.0$). The dashed line marks the time $t = T$ at which the second quench is performed; the rate function $l(t)$ is shown explicitly in Fig. 3(a) for the quench times $TJ = 0.5, 1, 2$ marked by dotted lines. We stress that kinks at times $t > T$ only occur for specific quench durations.

The rest of this paper is organized as follows: Section II gives a general introduction to the physical systems studied, the observables calculated, and the methods used. Section III summarizes our main results about the controllability of DQPT in both the transverse-field Ising model and the axial next-nearest-neighbor Ising (ANNNI) chain. In Sec. IV we analyze the connection between nonanalyticities in the rate function and the magnetization. Finally, in Sec. V we close with a concluding summary.

II. SETUP, MODEL, AND METHODS

A. Setup

We compute the return amplitude (1) and its corresponding rate function (2) for a time-dependent Hamiltonian $H(t)$ that models a double quantum quench

$$H(t) = \begin{cases} H_0, & t < 0, \\ H_1, & 0 \leqslant t \leqslant T, \\ H_2, & T < t. \end{cases} \tag{3}$$

As before, $|\Psi_0\rangle$ is the ground state of an initial Hamiltonian H_0.

B. Model

Specifically, we consider the following one-dimensional Hamiltonian:

$$H(\Delta, g) = -J \sum_i \left[\sigma_i^z \sigma_{i+1}^z + \Delta \sigma_i^z \sigma_{i+2}^z + g\sigma_i^x\right], \tag{4}$$

where $\sigma_i^{x,y,z}$ denotes Pauli matrices acting at site i. We assume $J > 0$ and $g \geqslant 0$, while Δ can be positive or negative. For $\Delta = 0$, one recovers the transverse-field Ising chain, which can be mapped to a system of free fermions and hence be solved exactly. The Ising chain exhibits a quantum phase transition [41] at $g_c = 1$, which separates a ferromagnetic (FM) phase for $g < 1$ from a paramagnetic (PM) phase for $g > 1$. In the thermodynamic limit, the FM possesses two degenerate ground states $|\pm\rangle$ with $\langle\sigma_i^z\rangle \neq 0$, while the PM ground state with $\langle\sigma_i^z\rangle = 0$ is unique.

For finite next-nearest-neighbor interactions $\Delta \neq 0$, one obtains the ANNNI chain [42,43]. The model can be mapped to a system of interacting fermions with interaction strength $\propto \Delta$, which can no longer be solved exactly. The phase diagram of this model has been studied by several methods [44–49]. In addition to the FM and PM it also possesses two additional phases at large, repulsive values of the interaction $\Delta > 1$.

For the rest of this paper, we will keep J fixed; our double quench is thus entirely determined by the three pairs of the values (Δ_m, g_m), $m = 0, 1, 2$, together with $H_m = H(\Delta_m, g_m)$.

C. Analytical approach

For the analytical approach we consider a chain of length L with periodic boundary conditions on the spin variables, $\sigma_{L+1}^a = \sigma_1^a$. Furthermore, we restrict ourselves to double quenches in the transverse-field Ising model ($\Delta_m = 0$), for which exact results can be obtained. To this end, we map the model to noninteracting fermions via a Jordan-Wigner transformation (see, e.g., Ref. [50], which we follow in our notation). In the fermionic language, the Hamiltonian can be diagonalized straightforwardly,

$$H(\Delta = 0, g) = \sum_k \epsilon_k(g) \left(\eta_k^\dagger(g)\eta_k(g) - \frac{1}{2}\right), \tag{5}$$

where

$$\epsilon_k(g) = 2J\sqrt{1 + g^2 - 2g\cos k}, \tag{6}$$

and $\eta_k^\dagger(g)$ and $\eta_k(g)$ are fermionic creation and annihilation operators. Depending on the filling fraction, the fermions fulfill either antiperiodic boundary conditions with the momenta quantized as half-integer multiples of $2\pi/L$, or periodic boundary conditions with the momenta quantized as integer multiples of $2\pi/L$. The antiperiodic case is usually referred to as the Neveu-Schwarz (NS) sector, while the periodic one is known as the Ramond (R) sector, respectively.

The initial state for the double-quench protocol is given by the unique ground state of the fermionic model $|0, g_0\rangle$, which lies in the NS sector for any finite system. For $g_0 > 1$ this corresponds to the unique PM ground state of the Ising model. We stress, however, that in the FM phase $0 \leqslant g < 1$ the fermionic ground state corresponds to a superposition of the magnetic states $|\pm\rangle$ [50].

The fermionic modes which diagonalize the Hamiltonian at different values of the transverse field are related via

$$\eta_k(g_1) = \cos\frac{\theta_k(g_2) - \theta_k(g_1)}{2}\,\eta_k(g_2) + \mathrm{i}\sin\frac{\theta_k(g_2) - \theta_k(g_1)}{2}\,\eta_{-k}^\dagger(g_2), \tag{7}$$

where the Bogoliubov angle $\theta_k(g)$ is determined from

$$e^{\mathrm{i}\theta_k(g)} = \frac{g - e^{\mathrm{i}k}}{\sqrt{1 + g^2 - 2g\cos k}}. \tag{8}$$

Using the relations (7) together with the fact that the initial state is the vacuum state, $\eta_k(g_0)|0,g_0\rangle = 0$, the rate function for the return probability for times $t < T$ is found to be [4]

$$l(t) = -\frac{1}{\pi}\int_0^\pi dk\ \ln\left|\cos^2\frac{\theta_k(g_1)-\theta_k(g_0)}{2} + \sin^2\frac{\theta_k(g_1)-\theta_k(g_0)}{2}\, e^{-2i\epsilon_k(g_1)t}\right|, \tag{9}$$

while for times $t > T$ we obtain

$$l(t) = -\frac{1}{\pi}\int_0^\pi dk\ \ln\left|A_k + B_k\, e^{-2i\epsilon_k(g_2)t}\right| + 2\ln 2. \tag{10}$$

The coefficients A_k and B_k depend on all quench parameters and are explicitly given by

$$\begin{aligned} A_k &= 1 + \cos[\theta_k(g_0)-\theta_k(g_1)] + \cos[\theta_k(g_0)-\theta_k(g_2)] \\ &\quad + \cos[\theta_k(g_1)-\theta_k(g_2)] + (1 - \cos[\theta_k(g_0)-\theta_k(g_1)] \\ &\quad + \cos[\theta_k(g_0)-\theta_k(g_2)] - \cos[\theta_k(g_1)-\theta_k(g_2)])e^{-2i\epsilon_k(g_1)T}, \end{aligned} \tag{11}$$

$$\begin{aligned} B_k &= (1 + \cos[\theta_k(g_0)-\theta_k(g_1)] - \cos[\theta_k(g_0)-\theta_k(g_2)] \\ &\quad - \cos[\theta_k(g_1)-\theta_k(g_2)])e^{2i\epsilon_k(g_2)T} \\ &\quad + (1 - \cos[\theta_k(g_0)-\theta_k(g_1)] - \cos[\theta_k(g_0)-\theta_k(g_2)] \\ &\quad + \cos[\theta_k(g_1)-\theta_k(g_2)])e^{-2i[\epsilon_k(g_1)-\epsilon_k(g_2)]T}. \end{aligned} \tag{12}$$

D. DMRG approach

In addition to the analytical approach discussed above, we employ the density matrix renormalization group [51–53] (DMRG) to study the double-quench setup. The reason for this is twofold: (1) The DMRG allows us to study quenches within the Ising chain that start from a polarized state, which is not a ground state of the fermionic model. Such quenches feature nontrivial dynamics of the magnetization and will be investigated in Sec. IV in detail. (2) One can treat the ANNNI chain [$\Delta \neq 0$ in Eq. (4)] which cannot be solved analytically; we will demonstrate that the picture described in Sec. III A persists in such a nonintegrable model.

At the technical level, we employ an infinite-system DMRG algorithm that is set up directly in the thermodynamic limit. We first determine the ground state using an evolution in imaginary time and then carry out a real-time evolution to compute the rate function $l(t)$. The discarded weight is kept constant during the latter, which leads to a dynamic increase of the bond dimension. We performed every calculation using various different values of the discarded weight in order to ensure convergence. Further details of the numerical implementation can be found in Ref. [7].

III. RESULTS

A. General observations

Let us first recall [6] how DQPTs manifest for single quenches (i.e., $T = \infty$) within the Ising chain ($\Delta_m = 0$). If the quench crosses the critical point $g = 1$, the rate function (2) exhibits kinks in its time evolution, while such nonanalytic behavior is not observed if both g_0 and g_1 belong to the same phase. (Note, however, that for other models the appearance of DQPTs is no longer tied to the fact whether or not the quench crossed a critical point [11].)

For the double-quench setup, we will demonstrate below that the appearance or absence of DQPTs not only depends on the values of the quench parameters but also dramatically on the time T between the first and the second quench. This entails a remarkable degree of controllability of the DQPTs. In fact, all four possible combinations for the absence or presence of kinks for times $t < T$ (after the first quench) and $t > T$ (after the second quench) can be realized. Strikingly, the existence of nonanalytic behavior in the rate function after the second quench can be tuned in a highly nonmonotonic fashion, where in a recurring manner the DQPTs can be suppressed and reinstated by increasing T.

For future reference, we label the four cases mentioned above as follows: The rate function shows (i) no nonanalyticities at all, (ii) no nonanalyticities for $t < T$ but kinks for $t > T$, (iii) nonanalyticities for $t < T$ but not for $t > T$, and (iv) kinks both for $t < T$ and $t > T$. The general observation that the appearance and absence of kinks can be tuned by varying T is condensed in Fig. 1, which shows the critical times t_n^* at which the rate function is nonanalytic in dependence of the time T for a typical set of parameters $g_0 = 1.5$, $g_1 = 0.5$, and $g_2 = 5.0$ in the Ising model (see Sec. III B for more details). Increasing T, we find recurring, discrete sets of lines of t_n^* (solid lines in Fig. 1) which extend into the regime $t > T$. This illustrates that the appearance and vanishing of DQPTs after the second quench can be tuned by changing T. For a given value of T, the critical times t_n^* at which rate function $l(t)$ shows kinks are determined by the crossing points of vertical lines in Fig. 1 with the solid ones. Tokens of the classes (i)–(iv) defined above are thus, e.g., $TJ = 0.5, 1, 2, 3.5$, respectively. The recurring appearance and suppression of DQPTs after the second quench suggests an intriguing fragility of the concept (in contrast to the quite robust equilibrium quantum phase transitions) and gives rise to the high susceptibility to tuning outlined above.

B. Analytic results for the Ising chain

The analytic results presented in Sec. II C allow us to obtain a complete understanding of the appearance of DQPTs for the transverse-field Ising chain. For times $t < T$, our setup is equivalent to the sudden quench protocol which was originally studied by Heyl *et al.* [6], who realized that the rate function $l(t)$ will show nonanalyticities at specific times t_n^* which are determined by a vanishing argument of the logarithm in Eq. (9). This happens if the quench crosses the quantum critical point, and the times t_n^* are located at [6]

$$t_n^* = \frac{\pi}{2\epsilon_{k^*}(g_1)}(2n+1), \quad n \in \mathbb{N}_0. \tag{13}$$

Here, the critical momentum k^* is obtained from the condition

$$\cot^2\frac{\theta_{k^*}(g_1)-\theta_{k^*}(g_0)}{2} = 1 \tag{14}$$

and explicitly given by $k^* = \arccos[(1+g_0g_1)/(g_0+g_1)]$. Depending on the value of T, one may thus observe a finite number of kinks before the second quench, as also shown in Fig. 1.

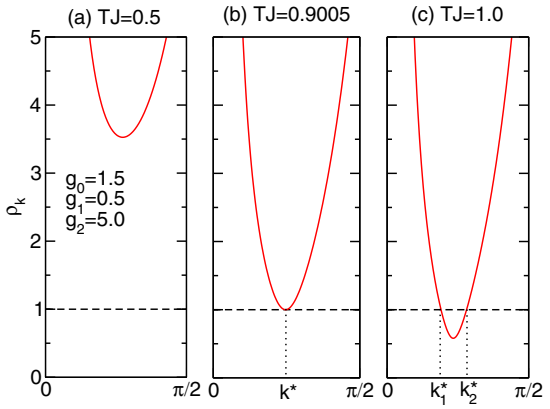

FIG. 2. Modulus $\rho_k = |A_k/B_k|$ for a double quench in the transverse-field Ising chain with quench parameters $g_0 = 1.5$, $g_1 = 0.5$, and $g_2 = 5.0$, and different quench times T. Generically we find either (a) no solution to (16), (b) one solution at $k = k^*$, or (c) two solutions $k = k^*_{1,2}$. Only the latter case results in critical times given by (17), at which the rate function shows nonanalytic behavior.

The situation becomes considerably more involved for times $t > T$, since Eq. (10) depends on all quench parameters g_0, g_1, and g_2 as well as the quench time T. To make our analysis more transparent, we will fix the values of the transverse field and discuss the dependence on T, also in light of the fact that this parameter can be directly controlled in experiments. As discussed above, nonanalyticities in the rate function (10) will appear whenever the argument of the logarithm vanishes,

$$\frac{A_k}{B_k} + e^{-2i\epsilon_k(g_2)} = \rho_k e^{i\varphi_k} + e^{-2i\epsilon_k(g_2)} = 0. \tag{15}$$

The main difference to the case $t < T$ is that due to the time evolution until $t = T$, the coefficient $A_k/B_k = \rho_k e^{i\varphi_k}$ is now no longer real but in general complex. It is thus reasonable to introduce the modulus ρ_k and the phase φ_k, for which the condition (15) implies

$$\rho_k = 1. \tag{16}$$

For double quenches starting and ending in the same phase (e.g., $g_0, g_2 > 1$, $g_1 < 1$), we generically find one of the three cases shown in Fig. 2: (a) There is no momentum for which Eq. (16) is satisfied; this is, for example, the case for quench times $TJ \lesssim 0.9$ or $2.97 \lesssim TJ \lesssim 3.92$ for the parameters shown in Fig. 1. The time evolution of the rate function is then completely analytic for all $t > T$. (b) There is one critical momentum k^* with $\rho_{k^*} = 1$, while for all other momenta we have $\rho_k > 1$. As we will discuss below, there are also no nonanalyticities in the time evolution in this case. (c) There are two critical momenta k_1^* and k_2^* at which Eq. (16) is satisfied. Close to these momenta, the function ρ_k is linear, which implies nonanalytic behavior of the rate function at times

$$t^*_{i,n} = \frac{\pi}{2\epsilon_{k_i^*}(g_2)}(2n+1) - \frac{\varphi_{k_i^*}}{2\epsilon_{k_i^*}(g_2)}, \tag{17}$$

where $i = 1,2$ and $n \in \mathbb{N}_0$. The phase shifts $\varphi_{k_i^*}$ originate from the time evolution for $t < T$. We note that while the individual sets $\{t^*_{i,n}\}$, $i = 1,2$ are periodic in time, due to the differing values of the prefactor $\pi/[2\epsilon_{k_i^*}(g_2)]$ the complete set of critical times $\{t^*_{1,n}\} \cup \{t^*_{2,n}\}$ is not periodic. In principle there may be more than two momenta at which (16) is satisfied, each of them giving rise to a set of critical times determined by (17).

The link between the cases (a)–(c) discussed here and the general cases (i)–(iv) introduced in Sec. III A is as follows: Depending on whether or not the critical times (13) appear up to T, the cases (a) and (b) result in the general cases (i) or (iii). Similarly, case (c) leads to cases (ii) or (iv).

Furthermore, the analytic result (10) allows us to analyze the behavior of the rate function close to the critical times (17). We expand the integrand around $k = k_i^*$ and $t = t^*_{i,n}$. As illustrated in Fig. 2(c), ρ_k is linear near k_i^*, $\rho_k \approx 1 + a(k - k_i^*)$, $a \in \mathbb{R}$, and thus we can approximate the rate function as follows:

$$l(t) \approx -\frac{1}{2\pi}\int_0^\pi dk\, \ln\left[a^2(k-k_i^*)^2 + (2\epsilon_{k_i^*}(g_2)\delta t)^2\right]$$
$$\approx \delta t = |t - t^*_{i,n}|. \tag{18}$$

This linear behavior seems to be a general feature of DQPTs; it was previously observed after quenches across the quantum critical point in the transverse-field Ising model [14] as well as the quantum Potts chain [28].

Finally, let us comment on the case where there is precisely one critical momentum k^*, as shown in Fig. 2(b). At this value,

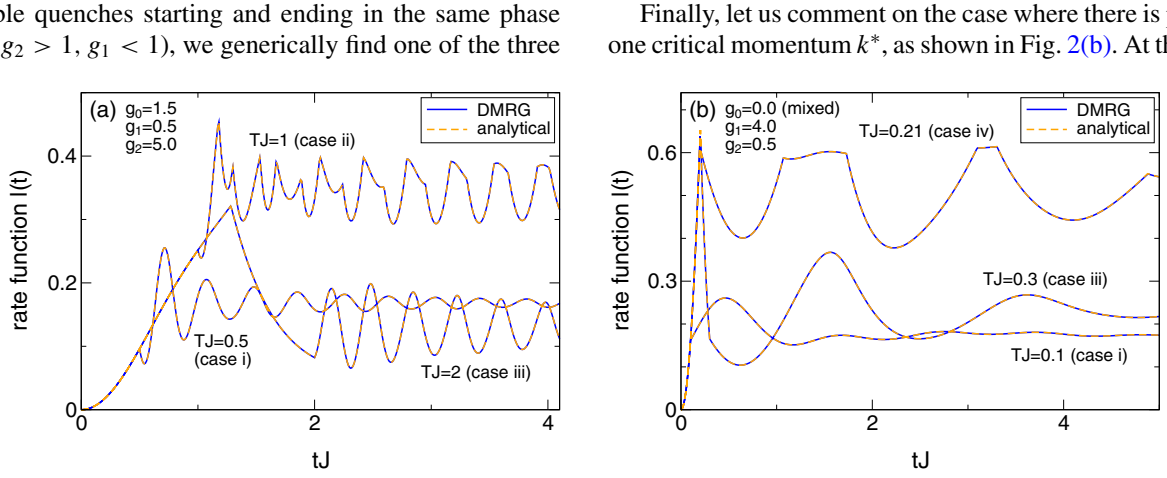

FIG. 3. Rate function $l(t)$ for a double quantum quench within the transverse-field Ising chain ($\Delta_m = 0$) for different quench times T and (a) quenches between the PM → FM → PM phases, and (b) quenches between the FM → PM → FM phases starting from a mixed FM state. We compare the exact analytical results derived in Sec. III B with those obtained from a DMRG calculation. By varying T, one can systematically tune the appearance and suppression of DQPTs after the second quench. The different possible cases are discussed in Sec. III A.

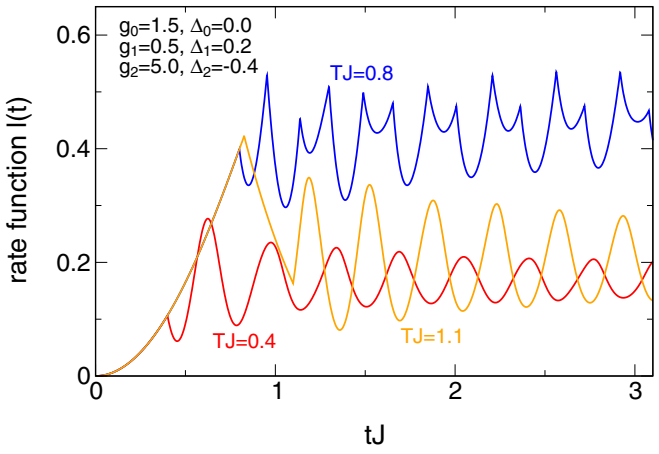

FIG. 4. Rate function for a double-quench PM → FM → PM with different quench times T for the ANNNI model. The results were obtained using DMRG.

the modulus ρ_k is no longer linear in $k - k^*$. Instead, we observe that when approaching the critical quench duration T_c (given by $T_c J \approx 0.9005$ for the parameters of Fig. 2) from above, the critical momenta $k^*_{1,2}$ and thus the times $t^*_{1,n}$ and $t^*_{2,n}$ approach each other, and eventually the kinks in the rate function simply disappear.

C. Numerical results for the ANNNI chain

We start by benchmarking our DMRG data for the Ising chain against the analytic results of Sec. II C. Figure 3 shows the rate function for two quenches starting from (a) the PM ground state and (b) the mixed FM ground state that corresponds to the NS state in the fermionic language. By varying the quench time T, one can realize each of the different cases discussed in Sec. III A. For example, for a quench starting in the mixed FM ground state [Fig. 3(b)], there are DQPTs for $TJ = 0.1$ (case i), for $TJ = 0.19$, kinks appear only for $t > T$ (case ii; not shown in the figure), for $TJ = 0.3$, there are kinks only for $t < T$ (case iii), and for $TJ = 0.21$, kinks appear for both $t < t$ and $t > T$ (case iv). In all cases, the DMRG data agree perfectly with the exact result.

Our general results, which we discussed in Sec. III A, were mainly based on the analytic solution of the transverse-field Ising model. It is important to show that the main conclusions are robust against breaking the integrability of this model and are therefore expected to hold in generic quantum many-body systems. To this end, in Fig. 4 we report results on the ANNNI model with finite Δ, which, to the best of our knowledge, is not integrable. We show that in complete analogy to the free (integrable) case, the behavior of the rate function $l(t)$ can be flexibly controlled by changing T; we explicitly demonstrate the appearance of the three cases: (i) no nonanalyticities ($TJ = 0.4$, red solid curve online), (ii) no nonanalyticities for $t < T$ but kinks for $t > T$ ($TJ = 0.8$, blue solid curve online), and (iii) nonanalyticities for $t < T$ but no kinks for $t > T$ ($TJ = 1.1$, orange solid curve online). While we cannot rule out that a different phenomenology emerges at larger times inaccessible to the DMRG, the data of Fig. 4 indicate that flexible control of the appearance of DQPTs is possible even in nonintegrable models; one can suppress and reestablish DQPTs at will.

IV. RELATION BETWEEN DQPTS AND MAGNETIZATION

By a remarkable experimental effort, the authors of Ref. [39] succeeded in directly measuring the rate function in a string of up to ten calcium ions, which are used to simulate long-ranged Ising models. Although a system of ten ions is admittedly small, the work established a connection between the theory of DQPTs and the nonequilibrium physics expected in real quantum simulators. In Ref. [39] also the magnetization was addressed for a quench starting from a FM polarized state, which is arguably a more natural quantity than the rate function. It was shown that the times where the magnetization vanishes are tied to the critical times t^*_n where kinks in the rate function show up. In Ref. [6], a similar connection was observed for the transverse-field Ising chain in the thermodynamic limit. In contrast, it was previously demonstrated that such a direct relation does *not* carry over to the nonintegrable case such as the ANNNI model [7]. This begs the question whether or not such a relationship between zeros in the magnetization and the critical times in the rate function exists for more general setups.

For the double quench, we observe that this is *not* the case (similarly to what is found for single quenches in nonintegrable models), suggesting that the correspondence is not robust (even for free models). In Fig. 5, we explicitly compare the rate function and the magnetization for a double quench starting from a FM polarized state of the transverse-field Ising model. The data was obtained using the DMRG method. One can explicitly see that the kinks in $l(t)$ at times $t > T$ after the second quench are in general *not* related to the zeros in the magnetization. This is most prominent in the $TJ = 0.58$ curve (dashed blue curve online), where the rate function for times $t > T$ shows repeated kinks, while the magnetization vanishes at a completely different time scale.

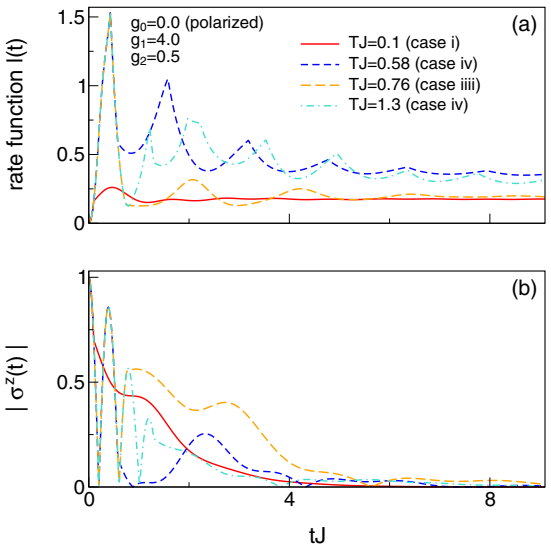

FIG. 5. (a) The same as in Fig. 3(b), but starting from a polarized FM state. (b) Behavior of the magnetization $|\langle\sigma^z(t)\rangle|$ during this type of quench. The data was computed using DMRG. We show that the times at which the magnetization vanishes are in general not tied to the critical times t^*_n where kinks in the rate function show up (in contrast to the transverse-field Ising chain).

V. CONCLUSION

In this paper, we have studied the phenomenon of DQPTs after double quantum quenches A → B → A between two equilibrium phases A and B. We have calculated the rate function analytically for the free transverse-field Ising chain. By varying the time T spent in phase B, one can control at will and in a recurring manner whether or not DQPTs occur after the second quench. All four possible combinations of the appearance and absence of nonanalyticities before and/or after the second quench can be realized if T is tuned. A similar picture emerges using finite-time DMRG numerics for the ANNNI model, which is a nonintegrable generalization of the Ising chain. Moreover, we demonstrated that even for the free transverse-field Ising chain there is no relationship between the critical times after the second quench and the zeros of the magnetization. In conclusion, our results show that the appearance of DQPTs is very fragile against the details of the quench setup.

ACKNOWLEDGMENTS

C.K. and D.K. are supported by the DFG via the Emmy-Noether program under KA 3360/2-1. D.S. is member of the D-ITP consortium, a program of the Netherlands Organization for Scientific Research (NWO) that is funded by the Dutch Ministry of Education, Culture and Science (OCW). D.S. was supported by the Foundation for Fundamental Research on Matter (FOM), which is part of the Netherlands Organization for Scientific Research (NWO) under 14PR3168.

[1] I. Bloch, J. Dalibard, and W. Zwerger, Rev. Mod. Phys. **80**, 885 (2008).
[2] *Atom Chips*, edited by J. Reichel and V. Vuletić (Wiley-VCH, Weinheim, 2011).
[3] A. Polkovnikov, K. Sengupta, A. Silva, and M. Vengalattore, Rev. Mod. Phys. **83**, 863 (2011).
[4] A. Silva, Phys. Rev. Lett. **101**, 120603 (2008).
[5] P. Calabrese and J. Cardy, Phys. Rev. Lett. **96**, 136801 (2006).
[6] M. Heyl, A. Polkovnikov, and S. Kehrein, Phys. Rev. Lett. **110**, 135704 (2013).
[7] C. Karrasch and D. Schuricht, Phys. Rev. B **87**, 195104 (2013).
[8] M. Heyl, Phys. Rev. Lett. **113**, 205701 (2014).
[9] E. Canovi, P. Werner, and M. Eckstein, Phys. Rev. Lett. **113**, 265702 (2014).
[10] J. M. Hickey, S. Genway, and J. P. Garrahan, Phys. Rev. B **89**, 054301 (2014).
[11] F. Andraschko and J. Sirker, Phys. Rev. B **89**, 125120 (2014).
[12] S. Vajna and B. Dóra, Phys. Rev. B **89**, 161105 (2014).
[13] J. N. Kriel, C. Karrasch, and S. Kehrein, Phys. Rev. B **90**, 125106 (2014).
[14] M. Heyl, Phys. Rev. Lett. **115**, 140602 (2015).
[15] S. Vajna and B. Dóra, Phys. Rev. B **91**, 155127 (2015).
[16] M. Schmitt and S. Kehrein, Phys. Rev. B **92**, 075114 (2015).
[17] S. Sharma, S. Suzuki, and A. Dutta, Phys. Rev. B **92**, 104306 (2015).
[18] A. J. A. James and R. M. Konik, Phys. Rev. B **92**, 161111 (2015).
[19] Z. Huang and A. V. Balatsky, Phys. Rev. Lett. **117**, 086802 (2016).
[20] U. Divakaran, S. Sharma, and A. Dutta, Phys. Rev. E **93**, 052133 (2016).
[21] J. C. Budich and M. Heyl, Phys. Rev. B **93**, 085416 (2016).
[22] N. O. Abeling and S. Kehrein, Phys. Rev. B **93**, 104302 (2016).
[23] S. Sharma, U. Divakaran, A. Polkovnikov, and A. Dutta, Phys. Rev. B **93**, 144306 (2016).
[24] T. Puškarov and D. Schuricht, SciPost Phys. **1**, 003 (2016).
[25] U. Bhattacharya, S. Bandyopadhyay, and A. Dutta, Phys. Rev. B **96**, 180303(R) (2017).
[26] B. Zunkovic, M. Heyl, M. Knap, and A. Silva, Phys. Rev. Lett. **120**, 130601 (2018).
[27] M. Heyl, Phys. Rev. B **95**, 060504 (2017).
[28] C. Karrasch and D. Schuricht, Phys. Rev. B **95**, 075143 (2017).
[29] S. A. Weidinger, M. Heyl, A. Silva, and M. Knap, Phys. Rev. B **96**, 134313 (2017).
[30] M. Heyl and J. C. Budich, Phys. Rev. B **96**, 180304 (2017).
[31] J. C. Halimeh and V. Zauner-Stauber, Phys. Rev. B **96**, 134427 (2017).
[32] V. Zauner-Stauber and J. C. Halimeh, Phys. Rev. E **96**, 062118 (2017).
[33] I. Homrighausen, N. O. Abeling, V. Zauner-Stauber, and J. C. Halimeh, Phys. Rev. B **96**, 104436 (2017).
[34] J. Lang, B. Frank, and J. C. Halimeh, Phys. Rev. B **97**, 174401 (2018).
[35] L. Piroli, B. Pozsgay, and E. Vernier, J. Stat. Mech. (2017) 023106.
[36] M. Heyl, F. Pollmann, and B. Dóra, arXiv:1801.01684.
[37] D. Trapin and M. Heyl, arXiv:1802.00020.
[38] L. Piroli, B. Pozsgay, and E. Vernier, arXiv:1803.04380.
[39] P. Jurcevic, H. Shen, P. Hauke, C. Maier, T. Brydges, C. Hempel, B. P. Lanyon, M. Heyl, R. Blatt, and C. F. Roos, Phys. Rev. Lett. **119**, 080501 (2017).
[40] N. Fläschner, D. Vogel, M. Tarnowski, B. S. Rem, D.-S. Lühmann, M. Heyl, J. C. Budich, L. Mathey, K. Sengstock, and C. Weitenberg, Nat. Phys. **14**, 265 (2018).
[41] S. Sachdev, *Quantum Phase Transitions* (Cambridge University Press, Cambridge, UK, 1999).
[42] W. Selke, Phys. Rep. **170**, 213 (1988).
[43] S. Suzuki, J. Inoue, and B. K. Chakrabarti, *Quantum Ising Phases and Transitions in Transverse Ising Models* (Springer, Heidelberg, 2013).
[44] P. Ruján, Phys. Rev. B **24**, 6620 (1981).
[45] I. Peschel and V. J. Emery, Z. Phys. B **43**, 241 (1981).
[46] D. Allen, P. Azaria, and P. Lecheminant, J. Phys. A **34**, L305 (2001).
[47] M. Beccaria, M. Campostrini, and A. Feo, Phys. Rev. B **73**, 052402 (2006).
[48] M. Beccaria, M. Campostrini, and A. Feo, Phys. Rev. B **76**, 094410 (2007).
[49] E. Sela and R. G. Pereira, Phys. Rev. B **84**, 014407 (2011).
[50] P. Calabrese, F. H. L. Essler, and M. Fagotti, J. Stat. Mech. (2012) P07016.
[51] S. R. White, Phys. Rev. Lett. **69**, 2863 (1992).
[52] S. R. White, Phys. Rev. B **48**, 10345 (1993).
[53] U. Schollwöck, Ann. Phys. **326**, 96 (2011).